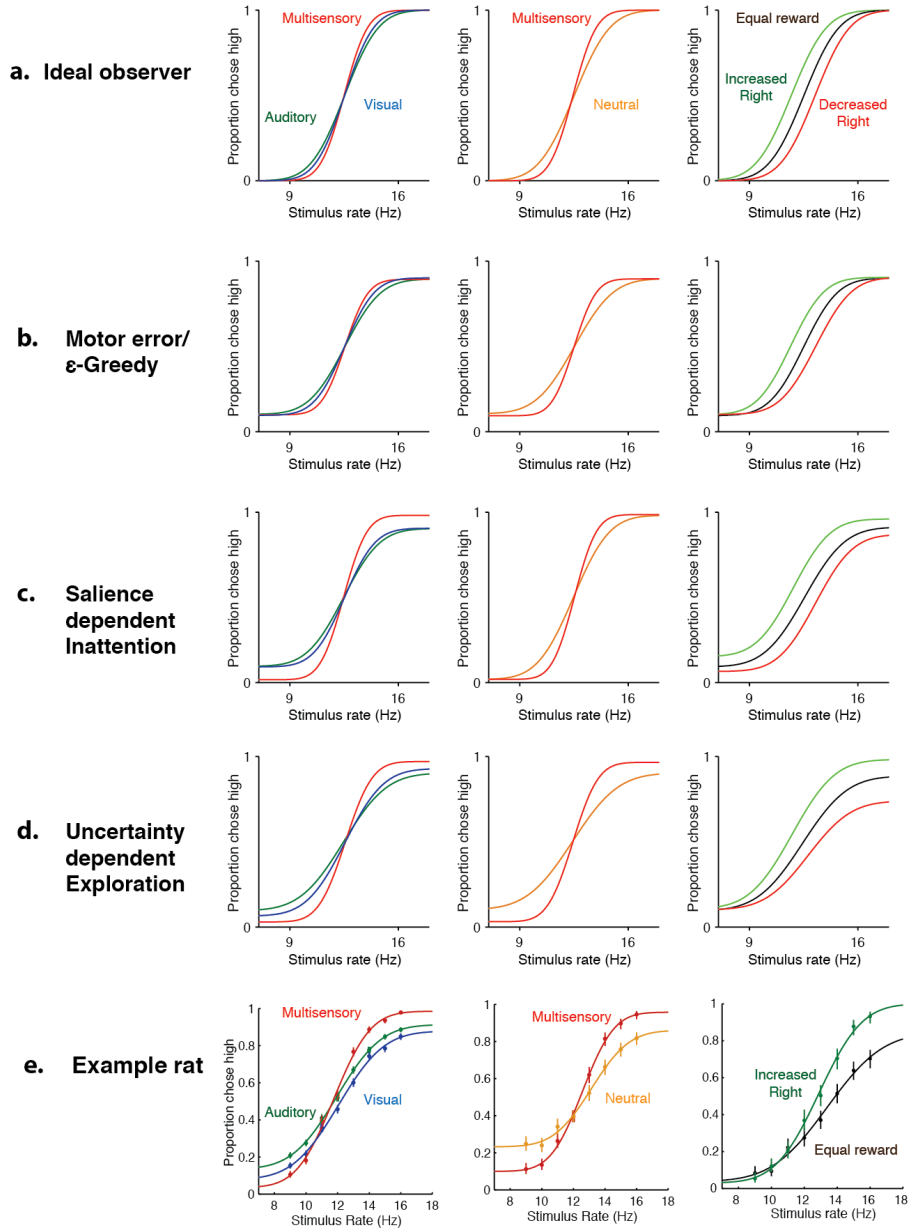


Supplementary figure 1

Schematic model predictions

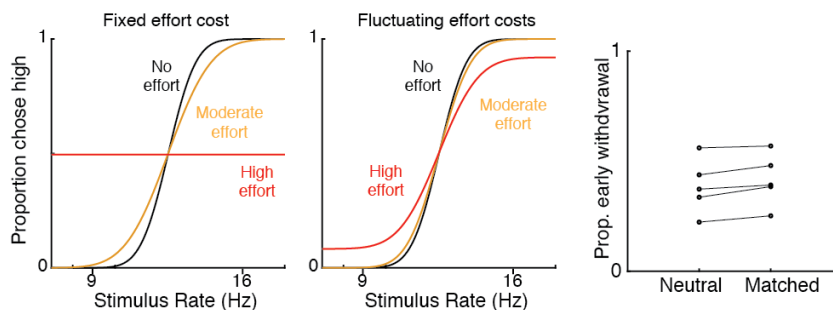


3 **Supplementary Figure 1: Uncertainty-dependent exploration is the only model that accounts for be-**  
 4 **havioral data from all three manipulations** Columns: data/predictions for three experimen-

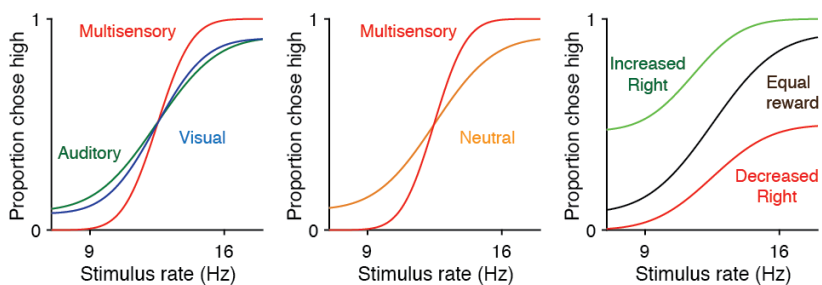
5 lations. Left: unisensory vs. multisensory. Middle: matched vs. neutral. Right: Asymmetric reward.  
6 a-d: Four candidate models. (a) Ideal observer model predicts no lapses and only changes in sensitiv-  
7 ity/bias across conditions. (b) Fixed motor error model predicts a constant rate of lapses across condi-  
8 tions in addition to changes in sensitivity/bias predicted from the ideal observer. (c) Inattention model  
9 predicts that the overall lapse rate (sum of lapses on both sides) depends on the level of bottom-up at-  
10 tentional salience, allowing for different rates for unisensory and multisensory. It also predicts that the  
11 lapse rate on neutral trials should be equal to that on multisensory trials, and that manipulating right-  
12 ward reward should affect both lapse rates. (d) Uncertainty-dependent exploration model predicts that  
13 overall lapse rate depends on the level of exploratoriness and hence uncertainty associated with that  
14 condition, allowing for different lapse rates on unisensory and multisensory trials. It also predicts that  
15 the lapse rate on neutral trials should be equal to that on auditory trials and manipulating rightward  
16 reward should only affect high rate lapses. (e) Data from an example rat on all three manipulations.

## Supplementary figure 2

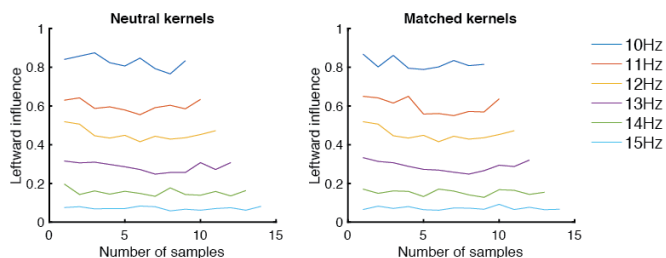
### a. Effort-dependent disengagement & guessing



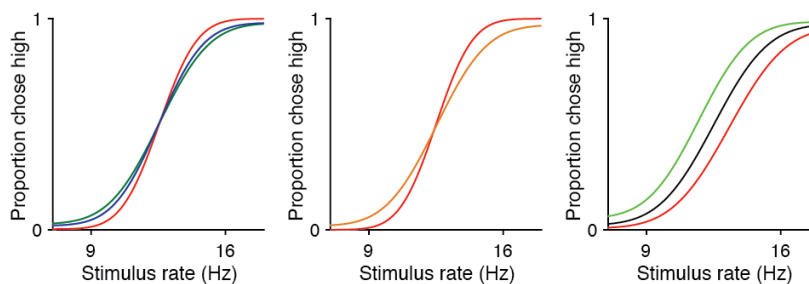
### c.



### d. Temporal inattention



### e. Variable precision

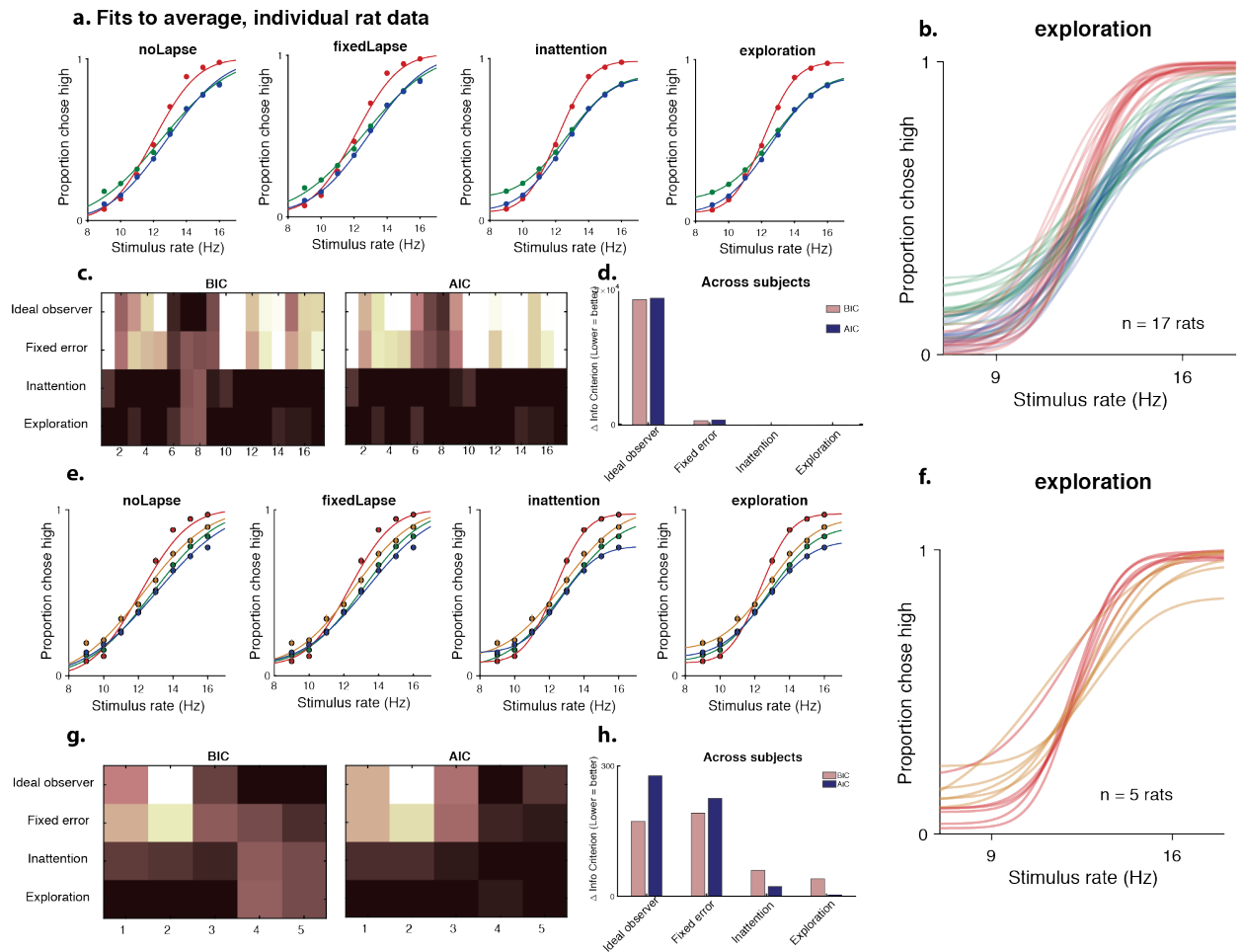


17

18 **Supplementary Figure 2: Alternative models of inattentional lapses.** Predictions of alternative models of  
 19 lapses. (a) Effort-dependent disengagement model: In this model, there is an additional cost or mental effort  
 20 to being engaged in the task which could vary with condition, and an additional random guessing action. If

21 the net payoff of engagement is not greater than the average value of a guess, then it guesses randomly. Such  
22 a model does not produce lapses if the effort is fixed across trials (left), but could produce lapses if the effort  
23 fluctuates from trial to trial (center). (b) Proportion of trials on which the animal withdrew prematurely doesn't  
24 vary between matched and neutral trials, suggesting that rats are not disengaging preferentially on neutral  
25 trials. (c) Predictions of the effort-dependent disengagement model. The model accurately predicts increased  
26 lapses on unisensory trials (left panel, green/blue traces) and neutral multisensory trials (middle panel, orange  
27 trace). However, for asymmetric reward manipulations (right), the model fails to predict our behavioral  
28 observation (Fig. 4d) that only lapses on the manipulated side are affected. (d) Temporal inattention model:  
29 in this model, temporal weighting of evidence differs between matched and neutral trials. To test this, we  
30 compared psychophysical kernels on matched and neutral trials. The temporal dynamics of attention are  
31 unchanged between the two kinds of trials, arguing against the temporal inattention model. (e) Variable  
32 precision model: in this model, the sensory noise (or its inverse, precision) fluctuates from trial to trial. The  
33 model accurately predicts increased lapses on unisensory trials (left panel, green/blue traces) and neutral  
34 multisensory trials (middle panel, orange trace). However, for asymmetric reward manipulations (right),  
35 the model fails to predict our behavioral observation (Fig. 4d) that lapses only on the manipulated side are  
36 affected. Like other models of inattention, it predicts that manipulating reward on one side should affect both  
37 lapses.

### Supplementary figure 3



38

39 **Supplementary Figure 3: Uncertainty guided exploration outperforms competing models for average**

40 **and individual data** (a) Fits of the four models to average rat data on unisensory (blue-visual, green-auditory)

41 and multisensory (red) trials. (b) Exploration model fits to unisensory and multisensory data for 17 individual

42 animals (c) Model comparison for individual animals using BIC (left), AIC (right). Darker colors are lower

43 BICs/AICs, denoting a better fit. (d) Summed model comparison metrics across animals, showing that

44 inattention and exploration models fit the data equally well, and much better than the ideal observer or fixed

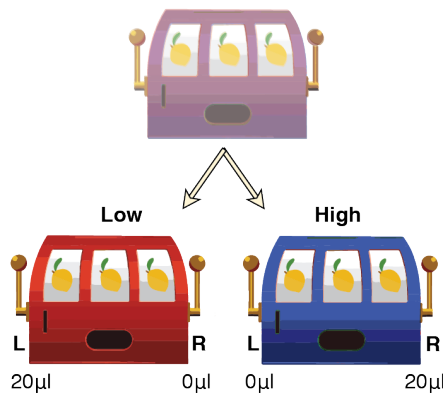
45 error models. (e) Fits of the four models to average data including neutral trials (orange) provide a stronger

46 test of the inattention model. (f) Exploration model fits to multisensory data including neutral trials for 5

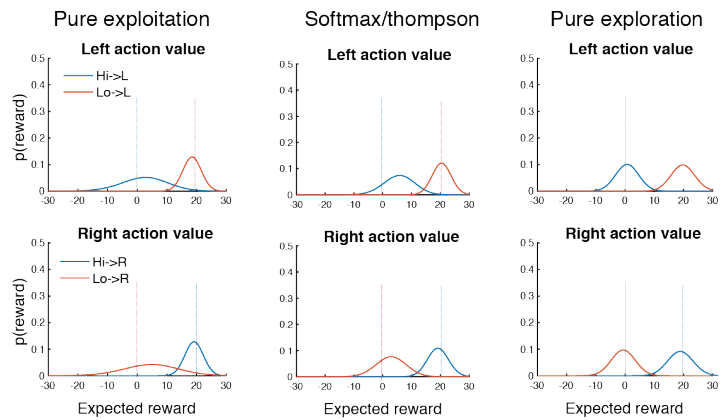
47 individual animals (g) Model comparison for individual animals. (h) Summed model comparison metrics  
 48 across animals shows that the uncertainty-guided exploration model performs better than other models.  
 49

**Supplementary figure 4**

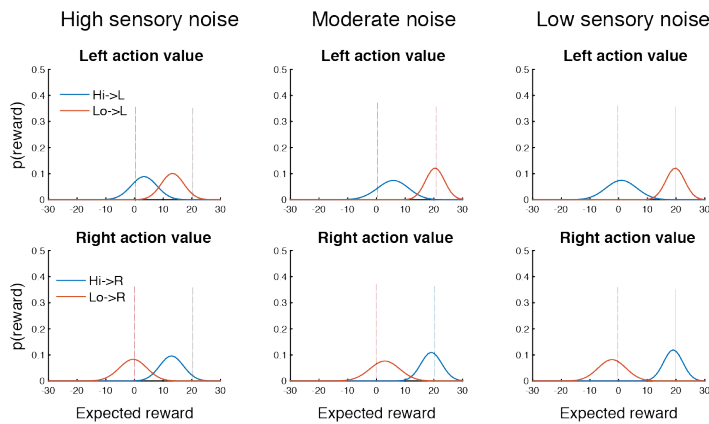
**a. Perceptual discrimination task**



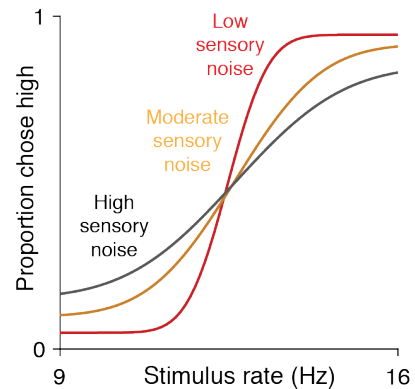
**b. Exploration-exploitation tradeoff**



**c. Dependence of value beliefs on sensory noise**



**d. Simulated performance**

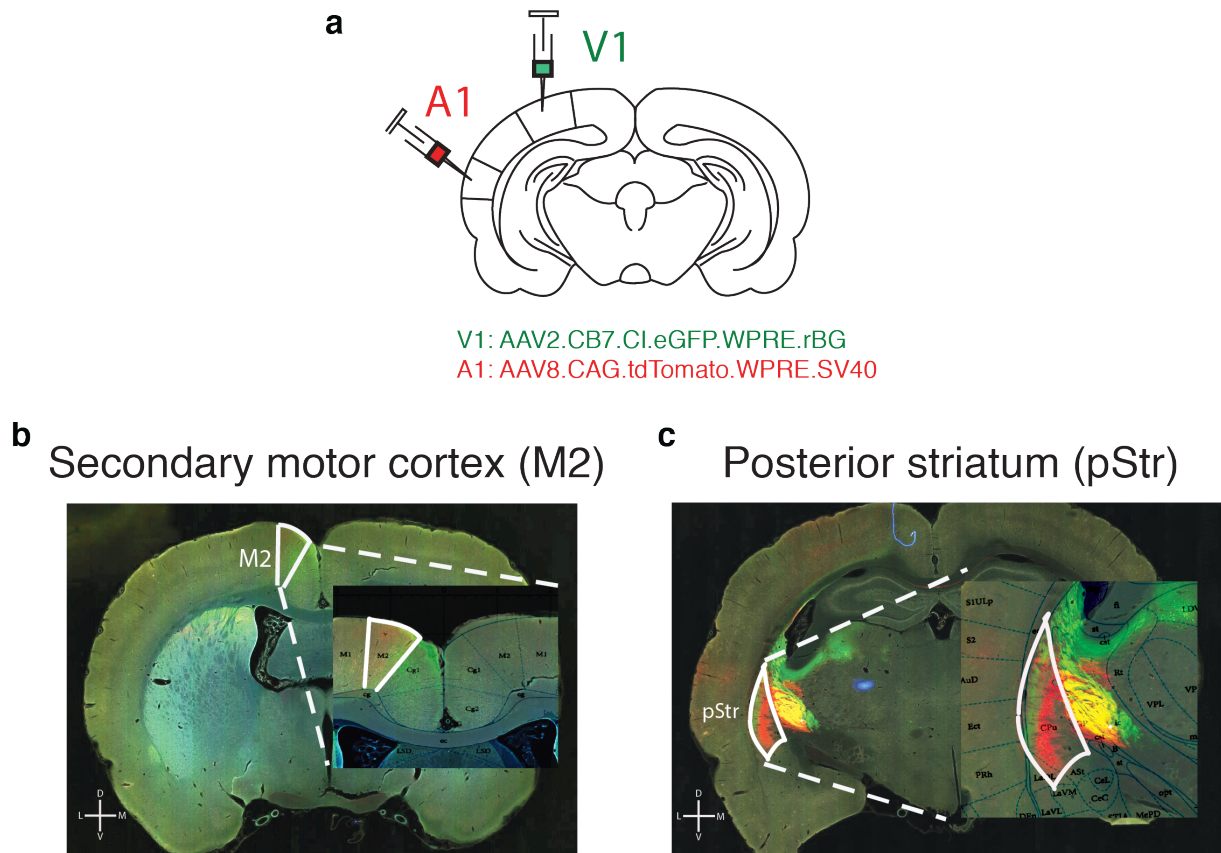


50

51 **Supplementary Figure 4: Thompson sampling, which balances exploration and exploitation, predicts**  
 52 **lapses that increase with perceptual noise** Schematic illustrating the explore-exploit tradeoff in perceptual  
 53 two-alternative tasks. (a) Formulation of perceptual decision making task as a partially observable contextual  
 54 bandit. To solve this task, an observer needs to infer the true category of the stimulus (Low or High) based

55 on noisy observations, and pick the best action given the true category (Left for Low, Right for High). This  
56 requires accurately learning the expected rewards from all 4 state-action pairs. (b) Beliefs about expected re-  
57 ward from different actions (L,R) performed in different states (Hi, Lo) showing different levels of uncertainty  
58 depending on policy. Beliefs are updated based on outcomes using a Bayesian update rule that takes into  
59 account uncertainty in state estimation. A greedy policy (left) that always picks the best action maximizes  
60 reward and learns well about the preferred state-action pairs (i.e. Lo-L and Hi-R) but has high uncertainty  
61 about the non-preferred pairs (Lo-R, Hi-L). A random policy (right) earns reward at chance, but learns  
62 equally well about all state-action pairs. Thompson sampling (center) implements a softmax decision rule that  
63 depends on the current uncertainties in each value, and balances immediately reward-maximizing decisions  
64 with decisions that reduce uncertainty, maximizing average reward in the long term. (c) Learnt beliefs about  
65 expected reward with Thompson sampling at various levels of perceptual uncertainty. High sensory noise  
66 (left) leads to large perceptual uncertainty, yielding highly overlapping belief distributions owing to a reduced  
67 ability to assign obtained rewards to one of the states. Lower levels of sensory noise (center, right) produce  
68 more separable beliefs. (d) Simulated performance over 2000 trials of the Bayesian learner shown above,  
69 under a Thompson sampling policy. As the sensory noise decreases (Black to Yellow to Red), the observer  
70 makes fewer exploratory choices owing to the more separable value beliefs, giving rise to lower lapse rates.

## Supplementary figure 5



71

72 **Supplementary Figure 5: pStr and M2 receive direct projections from visual and auditory cortex** (a)

73 Schematic of tracing experiments. AAV2.CB7.Cl.eGFP.WPRE.RBG and AAV2.CAG.tdTomato.WPRE.SV40

74 constructs were injected unilaterally to primary visual (V1) and auditory (A1) cortices, respectively (V1

75 coordinates: 6.9 mm posterior to Bregma; 4.2 mm to the right of midline; A1 coordinates: 4.7 mm posterior

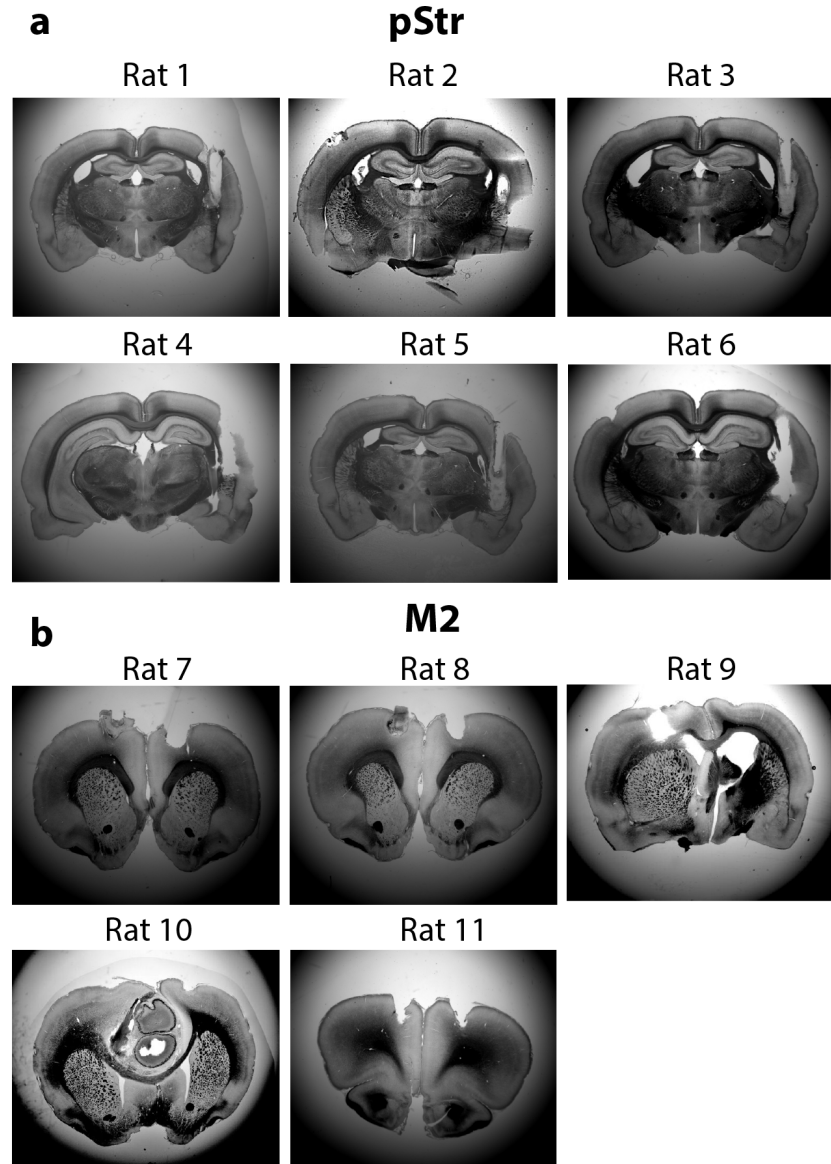
76 to Bregma; 7 mm to the right of midline). (b) Secondary motor cortex (M2) receives inputs from V1 and A1

77 as shown by green and red fluorescence. (c) Posterior striatum (pStr) receives direct inputs from V1 and A1

78 as shown by green and red fluorescence. Yellow signal medial to pStr reflects overlapping passing fibers.



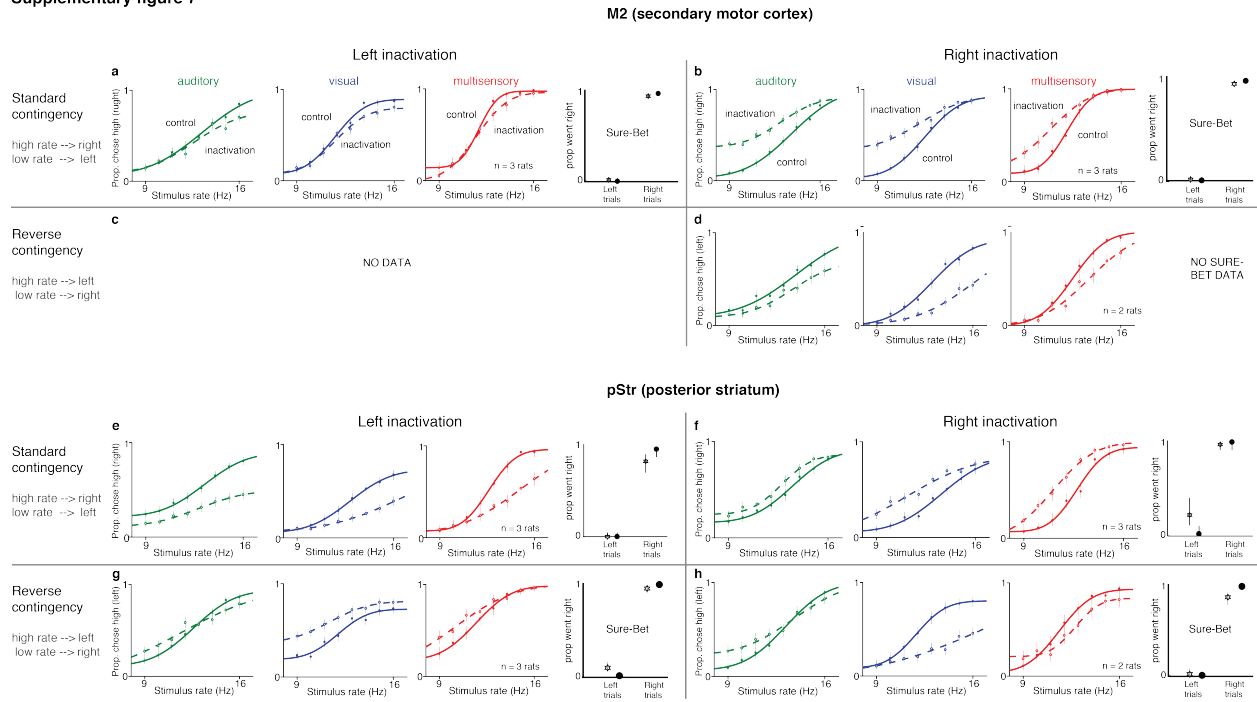
Supplementary figure 6



79

80 **Supplementary Figure 6: Histological slices of implanted rats** Representative coronal slices of all rats  
81 implanted with cannulae for muscimol inactivation experiments. (a) 6 rats were bilaterally implanted in  
82 posterior striatum (pStr). (b) 5 rats were implanted in secondary motor cortex (M2).

Supplementary figure 7



83

84 **Supplementary Figure 7: Unilateral inactivation of M2 or pStr biases performance ipsilaterally and**

85 **increases contralateral lapses** Performance of the same rats shown in Figure 5b depicted as a function of

86 the inactivated side (right or left) and the rate-contingency in which they were trained (standard or reverse).

87 Standard contingency: high rate = go right, low rate = go left; reverse contingency: high rate = go left, low

88 rate = go right. Each quadrant shows 4 plots: 3 psychometrics for rate discrimination trials and one for

89 performance on sure-bet trials. auditory (green), visual (blue) and multisensory (red). (a)-(d) M2 inactiva-

90 tion. (e)-(h) pStr inactivation. (a), (d) Rats trained on the standard contingency and inactivated on the left

91 hemisphere show increased lapses on the high rates (i.e., fewer rightward choices on high rates). No effect

92 on sure-bet trials. (b), (f) Rats trained on the standard contingency and inactivated on the right hemisphere

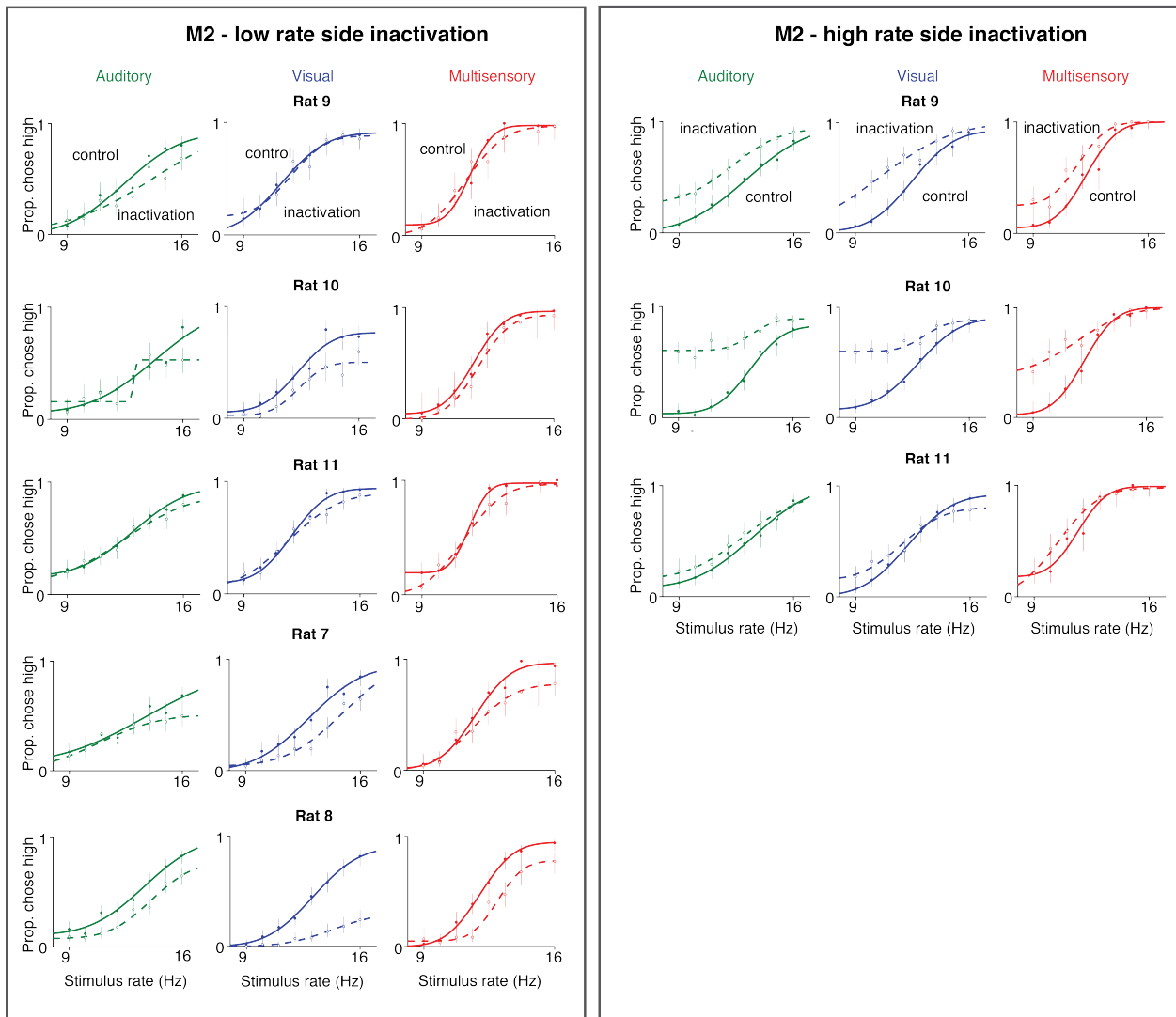
93 show increased lapses on the low rates (i.e., fewer leftward choices on low rates). No effect on sure-bet trials.

94 (c), (g) Rats trained on the reverse contingency and inactivated on the left hemisphere show increased lapses

95 on the low rates (i.e., fewer rightward choices on low rates). No effect on sure-bet trials. No data for this

96 condition for M2 inactivation. (d), (h) Rats trained on the reverse contingency and inactivated on the right  
 97 hemisphere show increased lapses on the high rates (i.e., fewer leftward choices on high rates). No effect on  
 98 sure-bet trials for pStr inactivated animals; no data for M2 inactivated animals.

99 **Supplementary figure 8**



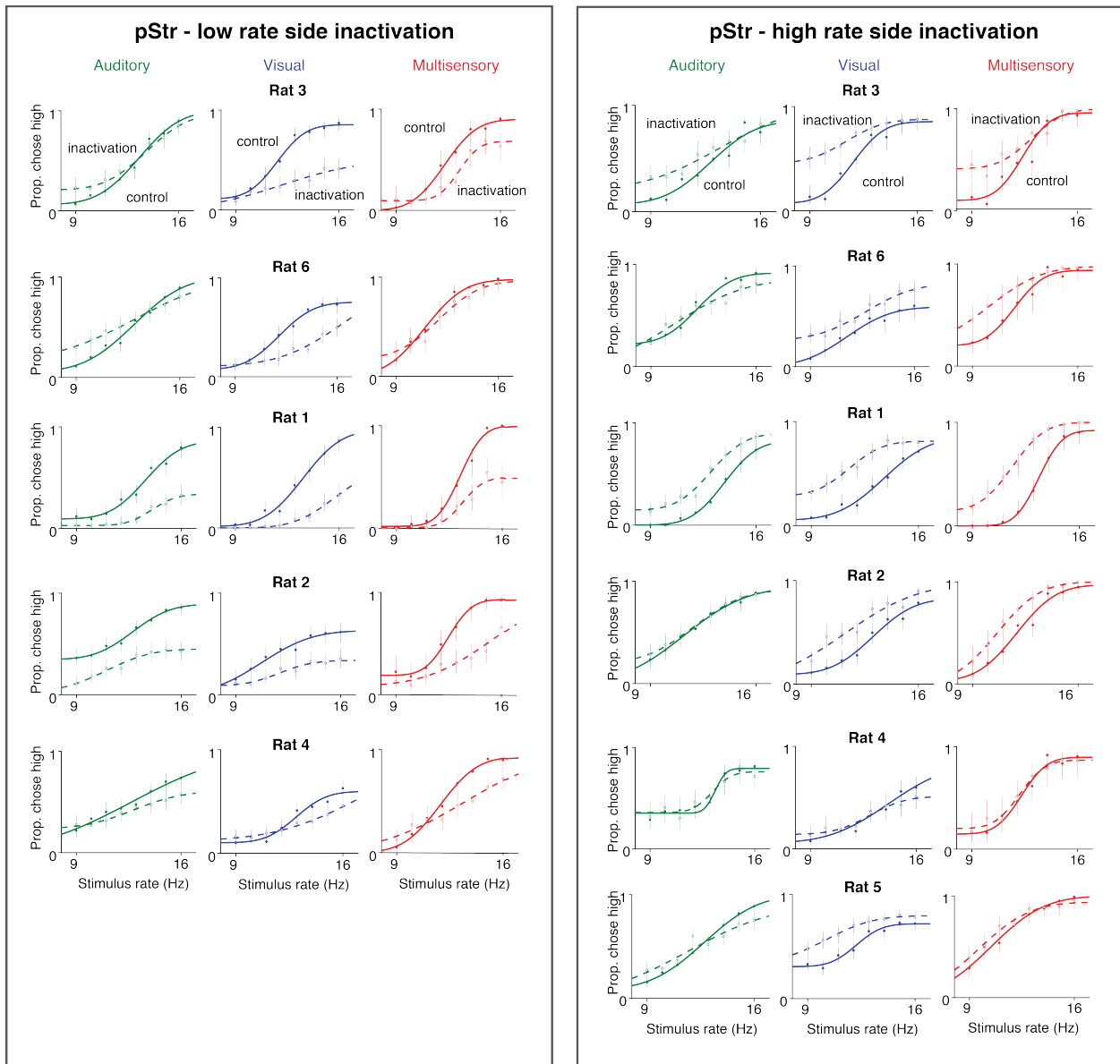
100

101 **Supplementary Figure 8: Single rat performance following M2 inactivation** Left: inactivation of the  
 102 low-rate associated side. Rat shows increased lapses on high-rate trials on all sensory modalities. Right:  
 103 inactivation of the high-rate associated side. Rat shows increased lapses on low-rate trials on all sensory

104 modalities. Auditory (green), visual (blue) and multisensory (red).

105

Supplementary figure 9



106

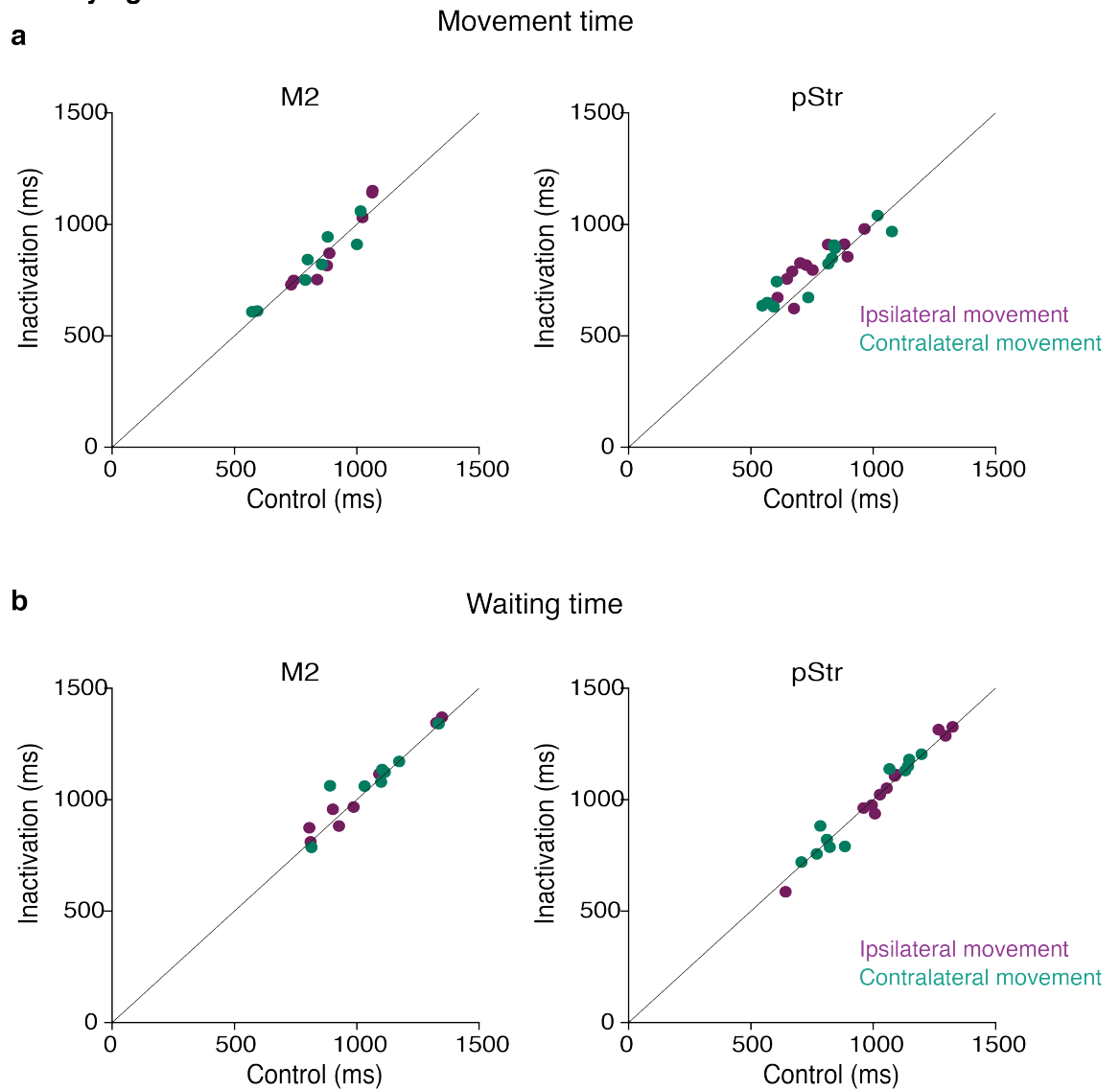
107 **Supplementary Figure 9: Single rat performance following pStr inactivation** Left: inactivation of the

108 low-rate associated side. Rat shows increased lapses on high-rate trials on all sensory modalities. Right:

109 inactivation of the high-rate associated side. Rat shows increased lapses on low-rate trials on all sensory

110 modalities. Auditory (green), visual (blue) and multisensory (red).

## Supplementary figure 10



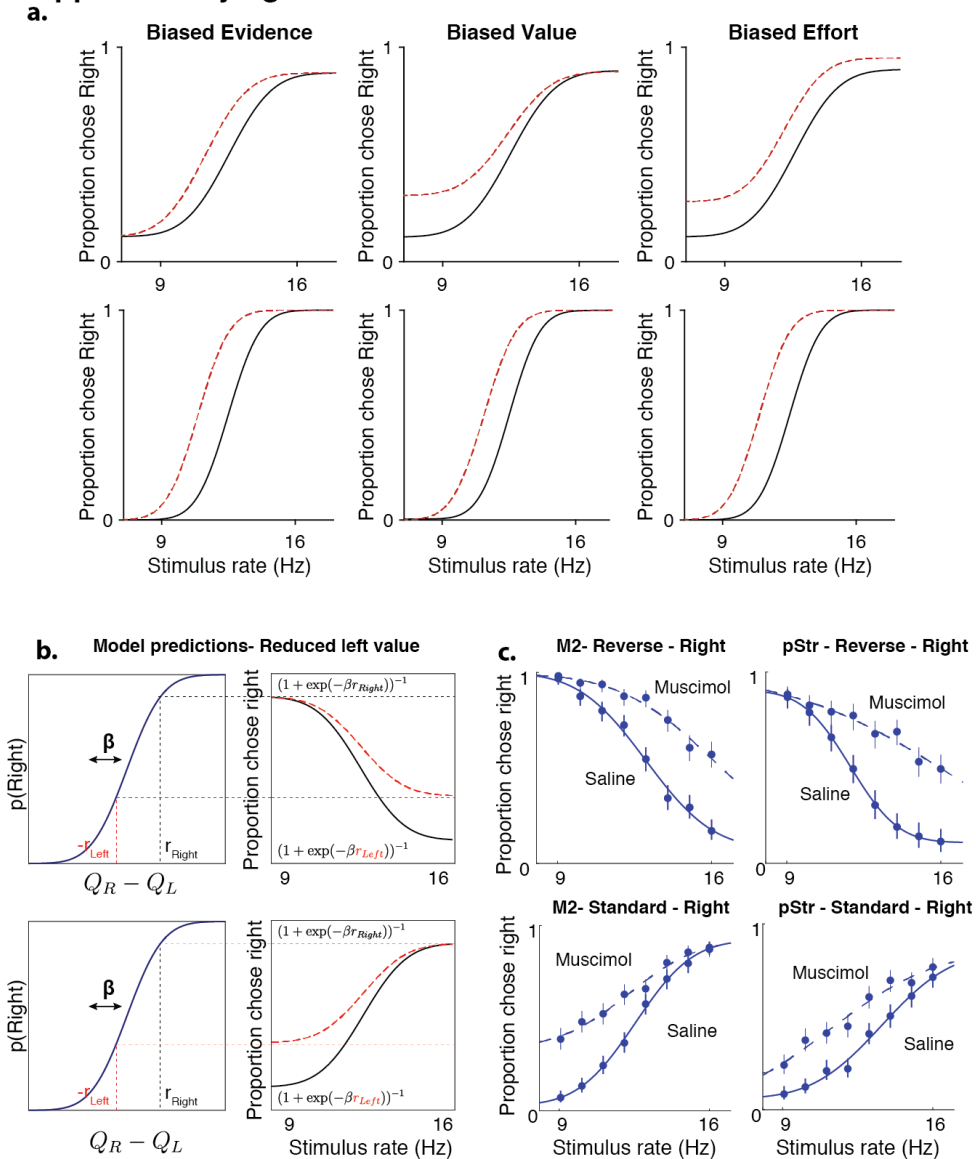
111

112 **Supplementary Figure 10: No significant effect on movement parameters following muscimol inacti-**  
113 **vation** (a) Mean movement times from the center port to the side ports were not significantly different  
114 following muscimol inactivation of M2 (left;  $p = 0.9554$  for contralateral,  $0.9852$  for ipsilateral movements;  
115  $n=5$  rats) or pStr (right;  $p = 0.6629$  for contra,  $p = 0.2615$  for ipsi,  $n=6$  rats). Control data on the abscissa  
116 is plotted against inactivation data on the ordinate. Purple, movement toward the side ipsilateral to the  
117 inactivation site; blue, movement toward the side contralateral to the inactivation site; Error bars (s.e.m.) are

118 not visible because they were obscured by the markers in all cases. (b) Mean wait times in the center port were  
 119 not significantly different following muscimol inactivation of M2 (left;  $p = 0.7612$  for contra,  $p = 0.8896$  for  
 120 ipsi,  $n=5$  rats) or pStr (right;  $p = 0.9128$  for contra,  $p = 0.9412$  for ipsi,  $n=6$  rats). All  $p$ -values were computed  
 121 from paired  $t$ -tests. Error bars (s.e.m.) are not visible because they were obscured by the markers in all cases.

122

**Supplementary figure 11**



123

124 **Supplementary Figure 11: Lapses differentiate perturbations to different stages of the decision-making**

125 **process** (a) Model predictions for biased sensory evidence (left), decreased contralateral action value (center)  
126 and increased effort in performing contralateral movements (right). The three kinds of perturbations affect  
127 decisions at the sensory, value or motor stages and predict different effects on lapses (top), but reduce to  
128 the same effect (horizontal shift) in the absence of lapses (bottom). (b) Model predictions for rightward  
129 inactivations on standard (top) and reversed (bottom) contingencies - in both cases, the model predicts that  
130 reduced leftward action values should only affect lapses on the side associated with leftward movements.  
131 (c) Inactivation data on visual trials from M2 (left) or pStr (Right) shows a pattern of effects consistent with  
132 action value deficits, irrespective of the stimulus-response contingency.